

Evidence for the $J^P = 1/2^+$ narrow state at 1650 MeV in the photoproduction of $K\Lambda$

T. Mart

Departemen Fisika, FMIPA, Universitas Indonesia, Depok 16424, Indonesia

(Dated: October 11, 2018)

Abstract

We have investigated the existence of the $J^P = 1/2^+$ narrow resonance predicted by the chiral soliton model by utilizing the kaon photoproduction process $\gamma + p \rightarrow K^+ + \Lambda$. For this purpose we have constructed two phenomenological models based on our previous effective Lagrangian model, which are able to describe kaon photoproduction from threshold up to $W = 1730$ MeV. By varying the mass (width) of an inserted P_{11} resonance from 1620 to 1730 MeV (0.1 to 1 MeV and 1 to 10 MeV) a number of fits has been performed in order to search for the resonance mass. Our result indicates that the most promising candidate mass (width) of this resonance is 1650 MeV (5 MeV). Although our calculation does not exclude the possibility of narrow resonances with masses of 1680, 1700 and 1720 MeV, the mass of 1650 MeV is obtained for all phenomenological models used in this investigation. Variations of the resonance width and $K\Lambda$ branching ratio are found to have a mild effect on the χ^2 . The possibility that the obtained result originates from other resonance states is also discussed.

PACS numbers: 13.60.Le, 13.30.Eg, 25.20.Lj, 14.20.Gk

I. INTRODUCTION

The ten members of the antidecuplet baryons predicted by the chiral quark soliton model (χ QSM) have drawn considerable attention for more than a decade. According to their strangeness and isospin these baryons can be organized as in Fig. 1. Among them three are exotic in the sense that their quantum numbers can be only built from 5 quarks, whereas the simplest states are clearly the two nonstrange nucleon resonances with $J^P = 1/2^+$ indicated by $N(1710)$ in the figure. It is interesting to learn that the mass of 1710 MeV was originally assigned by Diakonov, Petrov, and Polyakov [1] to these nonstrange antidecuplet members since at the time the Particle Data Group (PDG) [3] reported the resonance partial decay widths similar to those predicted by the χ QSM, i.e., strong decay to the ηN channel, whereas decays to the πN and $K\Lambda$ channels are relatively small, but comparable. Moreover, the total width of the $P_{11}(1710)$ reported by the PDG was uncertain [3].

Immediately after experimental observations of the exotic baryons $\Xi_{3/2}$ [4] and Θ^+ [5] had been reported, Walliser and Kopeliovich [2] found that the mass splitting within the baryon antidecuplet in Ref. [1] is overestimated by more than a factor of 1.5. By taking into account the SU(3) configuration mixing Walliser and Kopeliovich obtained the mass of the P_{11} should be either 1650 MeV or 1660 MeV, depending on whether a certain symmetry breaker (called Δ in Ref. [2]) is considered or not, respectively. We note that the agreement with experimental data is significantly improved if the Δ symmetry breaker is included in the calculation. In other words, within the topological soliton model of Walliser and Kopeliovich, experimental data prefer 1650 MeV for the mass of the P_{11} .

Not long after the finding of Walliser and Kopeliovich, Diakonov and Petrov [6] reevaluated the mass of the $N^*(1710)$ in Ref. [1] by using masses of these exotic baryons as inputs. It was found that the mass of the nonstrange member of this antidecuplet should be 1647 MeV if the possible mixing with lower-lying nucleonlike octet was not considered, but if the mixing was included the mass might shift upward to 1690 MeV. The width of the narrow resonance P_{11} was originally estimated to be 41 MeV [1]. However, from an analysis of the πN data, it was suggested the existence of a new narrow state $N^*(1680)$ with very small πN branching [7].

The large ηN branching ratio predicted by the χ QSM has sparked considerable interest in reevaluation of the η photoproduction at energies around 1700 MeV. It was then reported

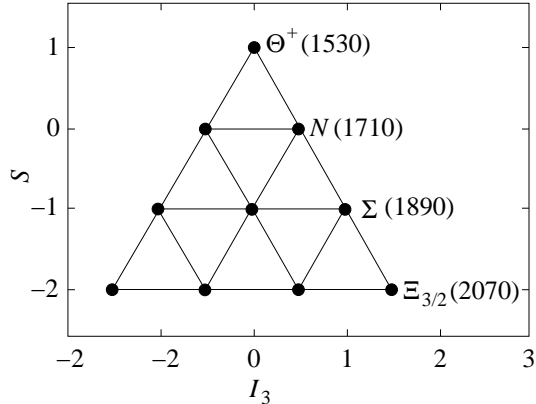


FIG. 1: Antidecuplet baryons predicted by the chiral soliton model [1].

that the cross section for the production off a free neutron is experimentally found to have a substantial enhancement at $W \approx 1670$ MeV [8]. This result has been confirmed by experiments of other collaborations [9]. Such enhancement is absent or very weak in the case of free proton. Clearly, the enhancement could be explained as the presence of the narrow P_{11} resonance [10]. However, different explanations are also possible. Within an SU(3) coupled channels model [11] the phenomenon can be described as the contributions of the $K\Lambda$ and $K\Sigma$ loops. Due to the cancellation with contributions from other channels, this cross section enhancement does not exist in the $\gamma p \rightarrow \eta p$ process. On the other hand, the Giessen group interpreted this enhancement as an interference effect between the $S_{11}(1650)$ and $P_{11}(1710)$ states [12]. The situation became more complicated as Ref. [13] found that this enhancement could be generated by other resonance states with different parities and spins.

In the πN sector there is only one notable study of this resonance [7]. In this study the narrow P_{11} mass is obtained from πN data by using a modified partial wave analysis (PWA), since the standard PWA can miss narrow resonances with $\Gamma < 30$ MeV [7, 14]. The changes in the total χ^2 were scanned in the range of resonance mass between 1620 to 1760 MeV after the inclusion of this resonance in the P_{11} partial wave. A clear effect was observed at 1680 MeV and a weaker one was detected at 1730 MeV. The same result was always obtained although the total width was varied between 0.1 and 10 MeV and branching ratio was also varied between 0.1 and 0.4.

To our knowledge there has been no attempt to study this resonance by utilizing kaon

photoproduction, although kaon photoproduction could offer a new arena for investigating this problem due to the explicit presence of strangeness in the final state. As stated above, the $N^* \rightarrow K\Lambda$ and $N^* \rightarrow \pi N$ branching ratios are predicted by the χ QSM to be comparable [1]. Partial wave analysis of the πN data yields the value of $\Gamma_{\pi N} = 0.5$ MeV, whereas theoretical analysis based on soliton picture results in $\Gamma_{K\Lambda} = 0.7$ (1.56) MeV for $m_{N^*} = 1680$ (1730) MeV [7]. In view of this we decide to follow the procedure developed in Ref. [7], i.e., we shall scan the changes in the total χ^2 after including a P_{11} narrow resonance with the variation of the resonance mass, width, and $K\Lambda$ branching ratio. Such a procedure is apparently suitable for kaon photoproduction, since the cross sections are relatively much smaller than in the case of πN or ηn , whereas the experimental error bars are in general relatively larger. As we can see in the next section, it is difficult to observe a clear structure in the cross sections at the energy of interest.

In spite of the difficult situation in kaon photoproduction, the accuracy of phenomenological model used in this study is crucial. Since the energy of interest is very close to the $K\Lambda$ threshold, an accurate model that can describe experimental data at low energies would be much better for this purpose, rather than a global model that fits to a wide energy range but tends to overlook the appearing small structures near threshold. Therefore, in this paper we shall start with the model developed in our previous analysis [15]. Because the model was constructed to explain experimental data only up to 50 MeV above the threshold, an extension of energy coverage is mandatory. In Ref. [7] the change of χ^2 was investigated up to $W = 1760$ MeV. Although we could in principle take 1760 MeV as the upper limit of our extended model, at $W \approx 1730$ MeV the problem of data discrepancy, between SAPHIR and CLAS data, starts to appear in the $K\Lambda$ photoproduction [16]. Extending the model beyond $W \approx 1730$ MeV results in a large χ^2 , which is obviously not suitable for the present purpose. On the other hand, as discussed above, Ref. [7] found that the most convincing mass of the narrow resonance is 1680 MeV. Therefore, we believe that it is sufficient to extend the model up to $W = 1730$ MeV and study the interval between threshold and $W \approx 1730$ MeV. This argument is also supported by the fact that no hadronic form factor is required to explain data up to this point, which is more favorable since it can simplify the reaction amplitudes and simultaneously reduce the number of uncertainties in the model. As shown in Ref. [17], the inclusion of this form factor leads to the problem of gauge invariance in the amplitude and, therefore, needs a proper treatment for restoring the gauge invariance.

This paper is organized as follows. In Section II we shall discuss the extension of our photoproduction model. Section III presents and discusses the result of our search for the narrow resonance. In Section IV, we give a brief discussion on the possibility that the obtained resonance is not a P_{11} state. In Section V we summarize our work and conclude our findings.

II. EXTENDING THE PHOTOPRODUCTION MODEL

A. The model

Our previous model [15] was constructed from the standard s -, u -, and t -channel Born terms along with the $K^{*+}(892)$ and $K_1(1270)$ t -channel vector mesons. To improve the agreement with experimental data, an $S_{01}(1800)$ hyperon resonance was also added to the background amplitude. In the s -channel term only the $S_{11}(1650)$ resonance state was included, since between threshold and the upper energy limit ($W = 1660$ MeV) only this resonance may exist. To facilitate the following discussion we need to present the corresponding resonant electric multipole from our previous analysis, i.e.,

$$E_{0+}(W) = \bar{E}_{0+} c_{K\Lambda} \frac{f_{\gamma R}(W) \Gamma_{\text{tot}}(W) m_R f_{KR}(W)}{m_R^2 - W^2 - im_R \Gamma_{\text{tot}}(W)} e^{i\phi}, \quad (1)$$

where $\bar{E}_{0+} = -A_{1/2}^{0+}$, W the total c.m. energy, Γ_{tot} the total width, m_R the physical mass, and ϕ the phase angle. The energy dependent partial width $\Gamma_{K\Lambda}$ is related to the single kaon branching ratio β_K via $\Gamma_{K\Lambda} = \beta_K \Gamma_R(|\mathbf{q}_K|/q_R)(W_R/W)$, with Γ_R and q_R the total width and kaon c.m. momentum at $W = m_R$, respectively. The explanation of other factors in Eq. (1) can be found in Ref. [15]. The available experimental data from threshold up to $W = 1660$ MeV were fitted by adjusting the coupling constants of the $K^{*+}(892)$, $K_1(1270)$, and $S_{01}(1800)$ intermediate states, as well as the phase angle ϕ of the $S_{11}(1650)$ resonance. Note that the older versions of SAPHIR data [18] were omitted from our database since the latest version [19] has better statistics and comes from the same experiment as the older ones. Furthermore, the leading coupling constants were fixed to the SU(3) prediction, i.e. $g_{K\Lambda N}/\sqrt{4\pi} = -3.80$ and $g_{K\Sigma N}/\sqrt{4\pi} = 1.20$, whereas except for the resonance phase angle, all resonance parameters of the $S_{11}(1650)$ were taken from the PDG values [20].

Compared to older analyses of kaon photoproduction, the result of the fits showed a much better agreement with experimental data considered. It was also found that the pseudoscalar

TABLE I: Properties of the nucleon resonances taken from the Review of Particle Properties [20].

Resonance	M_R (MeV)	Γ_R (MeV)	β_K	$A_{1/2}(p)$ ($10^{-3}\text{GeV}^{-1/2}$)	$A_{3/2}(p)$ ($10^{-3}\text{GeV}^{-1/2}$)	Overall status	Status seen in $K\Lambda$
$S_{11}(1650)$	1655^{+15}_{-10}	165 ± 20	0.029 ± 0.004	$+53 \pm 16$	-	****	***
$D_{15}(1675)$	1675 ± 5	150^{+15}_{-20}	< 0.01	$+19 \pm 8$	$+15 \pm 9$	****	*
$F_{15}(1680)$	1685 ± 5	130 ± 10	-	-15 ± 6	$+133 \pm 12$	****	
$D_{13}(1700)$	1700 ± 50	100 ± 50	< 0.03	-18 ± 13	-2 ± 24	***	**
$P_{11}(1710)$	1710 ± 30	100^{+150}_{-50}	0.15 ± 0.10	$+9 \pm 22$	-	***	**
$P_{13}(1720)$	1720^{+30}_{-20}	200^{+100}_{-50}	0.044 ± 0.004	$+18 \pm 30$	-19 ± 20	****	**

coupling yields a more significant improvement than the pseudovector one, especially in the case of the total and differential cross sections.

For the purpose of the present calculation we have to extend this model in order to take into account higher energy data since the χ QSM [1, 2] predicts the nonstrange member of the antidecuplet N^* to have a mass between 1650 and 1690 MeV. However, the latest calculation from the GWU group found that the most promising candidate mass is 1680 MeV, although another weak signal at 1730 MeV is not excluded. Therefore, it is sufficient to extend our previous model up to $W = 1730$ MeV. In the energy range between reaction threshold and 1730 MeV we observe that there exist 6 nucleon resonances listed in the recent Particle Data Book [20]. Their properties relevant to the present work are summarized in Table I.

We also note that there is no resonance state listed in the Particle Data Book between 1720 MeV and 1900 MeV. Therefore, we are convinced that it is sufficient to extend the model up to $W = 1730$ MeV. It is also important to mention here that the problem of data discrepancy between SAPHIR [19] and CLAS [22] data starts to appear at this energy (see Ref. [16] for a thorough discussion on this problem).

In the extended model we maintain the background terms as in our previous work [15], but in the resonance terms we include all six resonance states listed in Table I. Since the number of experimental data considered in the present work (704 points) is much larger than that in the previous work (139 points) it is important to relax the coupling constants restriction in order to achieve an acceptable χ^2 in our fits. Thus, for instance, we allow the main coupling

constants to vary within the allowed SU(3) values, assuming the SU(3) symmetry is broken at the level of 20%, i.e., $-4.4 \leq g_{K\Lambda N}/\sqrt{4\pi} \leq -3.0$ and $0.9 \leq g_{K\Sigma N}/\sqrt{4\pi} \leq 1.3$. At this stage it is important to note that in the energy of interest the hadronic form factors are not required for the background terms. This fact reduces the level of uncertainty and complexity in our model since the problem of gauge invariance due to the inclusion of hadronic form factors does not exist.

From Table I it is apparent that the values of photon helicity amplitudes $A_{1/2}$ and $A_{3/2}$ are unfortunately not accurate, in spite of the fact that the values directly control the magnitude of resonance contributions to the scattering amplitude as can be clearly seen in Eq. (1). In order that the results of the present work do not to dramatically differ from those of our previous analysis, where almost all resonance parameters were fixed to the PDG values, in the first model (Model 1) we restrict the maximum variation of the photon amplitudes during the fitting process to 10% of the original PDG values. In contrast to this, the variation of other parameters such as masses and total widths given in the Particle Data Book is mostly smaller than 10%. Therefore, in the latter we vary the parameters within the allowed values given in the Particle Data Book.

In the second model (Model 2) we do not constraint the variation of the resonance parameters as strict as in Model 1, i.e., all parameters are allowed to vary within the PDG error bars. Although we prefer Model 1 which retains the consistency with our previous analysis, Model 2 will be useful in the present work once we want to investigate the model dependence of the mass determination of the narrow resonance in the next section.

B. Numerical results and comparison with data

The numerical results of the fits are shown in Table II, where the background coupling constants of Kaon-Maid [21] are also listed for comparison. Obviously, the variation of the coupling constants between Model 1 and Model 2 is less dramatic than between the two models and Kaon-Maid. Nevertheless, except for the $G_{K^*}^T$ coupling, the sign of all coupling constants within the three models is clearly consistent. In the literature, the variation of these coupling constants is a long standing problem. Although Kaon-Maid was fitted to different experimental data set and has different resonance configuration as compared to the present work, Table II indicates that there is a tendency that the variation starts to

TABLE II: The extracted coupling constants of the present work (Model 1 and Model 2) compared with those of Kaon-Maid [21]. No hadronic form factors are used in both Model 1 and Model 2.

The number of data points used in both models is 704.

Fit parameters	Model 1	Model 2	Kaon-Maid
$g_{K\Lambda N}/\sqrt{4\pi}$	-3.00	-3.36	-3.80
$g_{K\Sigma N}/\sqrt{4\pi}$	1.30	1.30	1.20
$G_{K^*}^V/4\pi$	-0.46	-0.45	-0.79
$G_{K^*}^T/4\pi$	0.48	0.52	-2.63
$G_{K_1}^V/4\pi$	0.25	0.32	3.81
$G_{K_1}^T/4\pi$	-1.61	-1.36	-2.41
$G_{Y^*}/\sqrt{4\pi}$	-1.71	-1.06	-
$S_{11}(1650)$			
M (MeV)	1645	1670	-
Γ (MeV)	145	164	-
$A_{1/2}(10^{-3} \text{ GeV}^{-1/2})$	58	69	-
β_K	0.031	0.031	-
ϕ (deg)	176	195	-
$D_{15}(1675)$			
M (MeV)	1680	1670	-
Γ (MeV)	165	134	-
$A_{1/2}(10^{-3} \text{ GeV}^{-1/2})$	17	13	-
$A_{3/2}(10^{-3} \text{ GeV}^{-1/2})$	17	24	-
β_K	0.019	0.010	-
ϕ (deg)	11	34	-
$F_{15}(1680)$			
M (MeV)	1680	1680	-
Γ (MeV)	140	140	-
$A_{1/2}(10^{-3} \text{ GeV}^{-1/2})$	-17	-21	-
$A_{3/2}(10^{-3} \text{ GeV}^{-1/2})$	120	121	-
β_K	0.000	0.000	-
ϕ (deg)	185	219	-
$D_{13}(1700)$			
M (MeV)	1750	1675	-
Γ (MeV)	50	82	-
$A_{1/2}(10^{-3} \text{ GeV}^{-1/2})$	-19	-8	-
$A_{3/2}(10^{-3} \text{ GeV}^{-1/2})$	-2	22	-
β_K	0.050	0.010	-
ϕ (deg)	107	191	-

converge.

TABLE II: The extracted coupling constants of the present work (Model 1 and Model 2) compared with those of Kaon-Maid [21] (continued).

Fit parameters	Model 1	Model 2	Kaon-Maid
$P_{11}(1710)$			
M (MeV)	1690	1699	-
Γ (MeV)	98	174	-
$A_{1/2}(10^{-3} \text{ GeV}^{-1/2})$	10	31	-
β_K	0.140	0.140	-
ϕ (deg)	88	98	-
$P_{13}(1720)$			
M (MeV)	1700	1700	-
Γ (MeV)	150	150	-
$A_{1/2}(10^{-3} \text{ GeV}^{-1/2})$	16	18	-
$A_{3/2}(10^{-3} \text{ GeV}^{-1/2})$	-21	-39	-
β_K	0.048	0.048	-
ϕ (deg)	195	191	-
χ^2	859	704	-

Contribution of the background and resonance terms in the two models are exhibited in Fig. 2. It is obvious that the characteristic of resonance contributions can be comprehended from the values of kaon branching ratio β_K and photon helicity amplitudes $A_{1/2}$ and $A_{3/2}$ given in Table II. The two models show the same dominance of the background terms and the same large contribution of the $S_{11}(1650)$ resonance. The differences between them appear at relatively higher energies. The background contribution of Model 2 is somewhat suppressed at this kinematics in order to compensate contributions of the $S_{11}(1650)$, $P_{11}(1710)$ and $P_{13}(1720)$ resonances that tend to increase. From Fig. 2 (as well as Table II) it is also seen that the peak of the $S_{11}(1650)$ contribution is shifted to higher energy in Model 2. It is obvious that Model 1 is more consistent with our previous multipole analysis [16], i.e., the $S_{11}(1650)$ resonance contributes significantly, in contrast to the $P_{11}(1710)$.

A comparison between the predicted total cross section from the two models as well as from the Kaon-Maid and the available experimental data from SAPHIR [19] and CLAS [22] collaborations is shown in Fig. 3. It is clear that both Model 1 and Model 2 show a better agreement than the Kaon-Maid, although at very high energy (≥ 1.730 GeV) the total cross section predicted by Model 1 starts to increase, in contrast to the prediction of Model 2. This is understood from the fact that at this energy regime contribution of the background

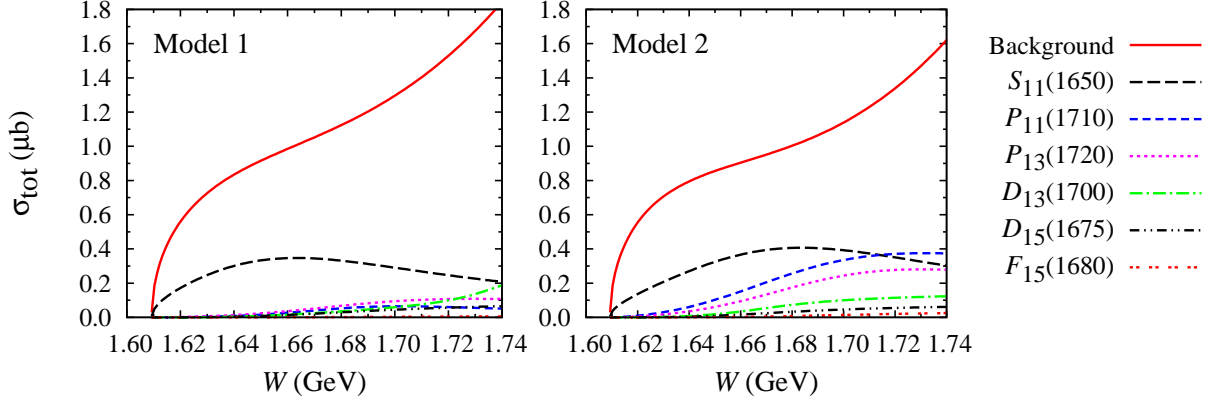


FIG. 2: (Color online) Contribution of the background and resonance terms to the total cross section for the two models used in the present work.

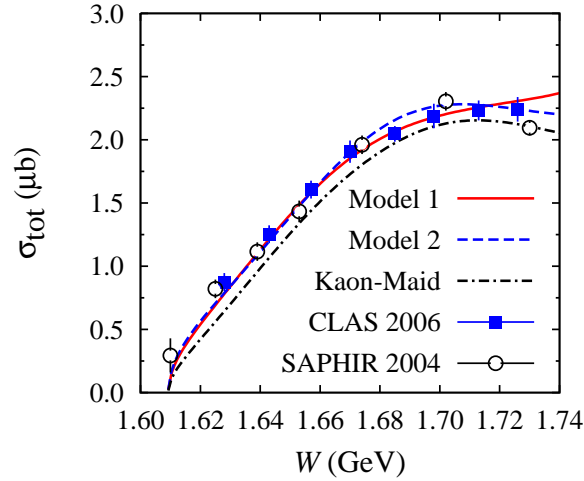


FIG. 3: (Color online) Comparison between total cross sections calculated from the Model 1, Model 2, and Kaon-Maid [21] with the available experimental data from the SAPHIR [19] and CLAS [22] collaborations. Note that error bars are statistical only and all data shown in this figure were not used in the fitting process.

terms in Model 1 is substantially larger than that in Model 2.

The angular distribution of the calculated differential cross sections is exhibited in Fig. 4. Within the error bars of the available experimental data we can say that all models work nicely in this case. Ideally, a full angular distribution of experimental data, such as the SAPHIR one, is desired for improving the model. Unfortunately, at forward angles SAPHIR

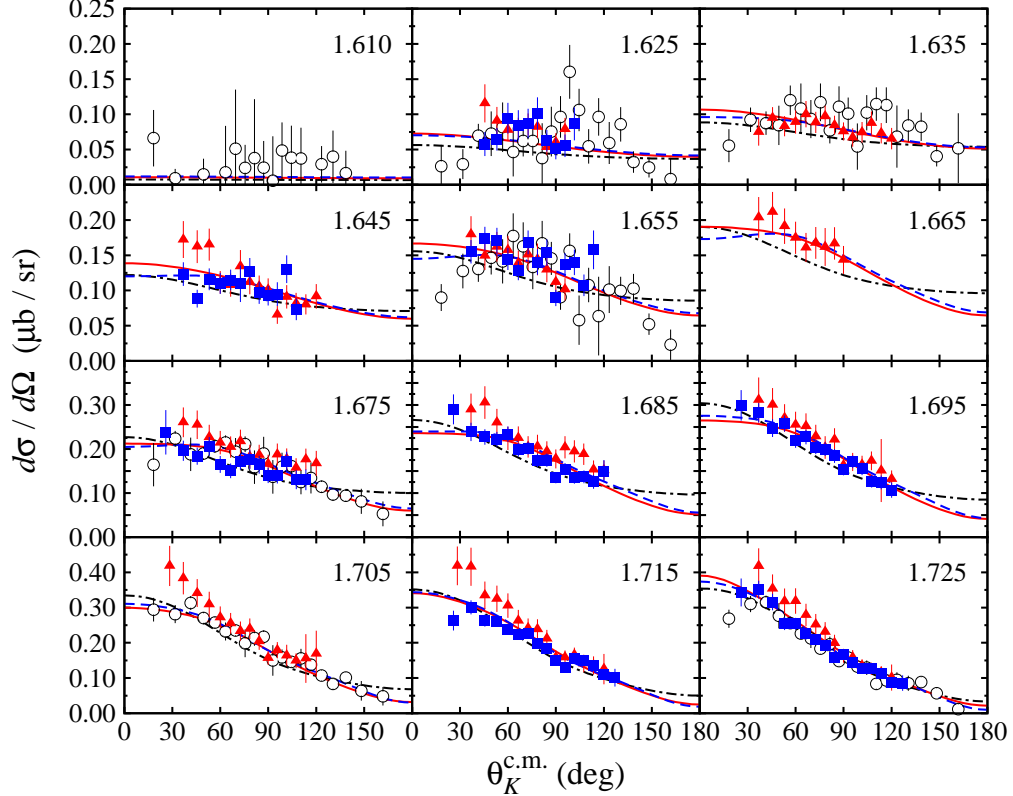


FIG. 4: (Color online) Comparison between angular distributions of differential cross section calculated from the Model 1, Model 2, and Kaon-Maid [21] with experimental data from the SAPHIR (open circles) [19], CLAS2006 (solid squares) [22] and CLAS2010 (solid triangles) [26] collaborations. The corresponding total c.m. energy W (in GeV) is shown in each panel. Experimental data displayed in this figure were used in the fits. Notation of the curves is as in Fig. 3.

data differ from CLAS data (see, e.g., panels with $W = 1.705$ and 1.715 GeV). Our models tend to approach the SAPHIR data, presumably due to their smaller error bars. In the case of Kaon-Maid model, the agreement with SAPHIR data is understandable because the model was fitted to the previous version of SAPHIR data [27], which are still consistent with the later version [19].

The energy distribution of differential cross sections for 20 different angle bins is shown in Fig. 5. The calculated cross sections of Model 1 and Model 2 are almost identical except at very forward angles and near $\theta_K^{\text{c.m.}} \approx 90^\circ$ with $W \geq 1.730$ GeV. The agreement of both models with experimental data is clearly better than in the case of Kaon-Maid. Although the experimental data do not show a clear resonance-like structure, a slight bump at $W \approx 1.690$

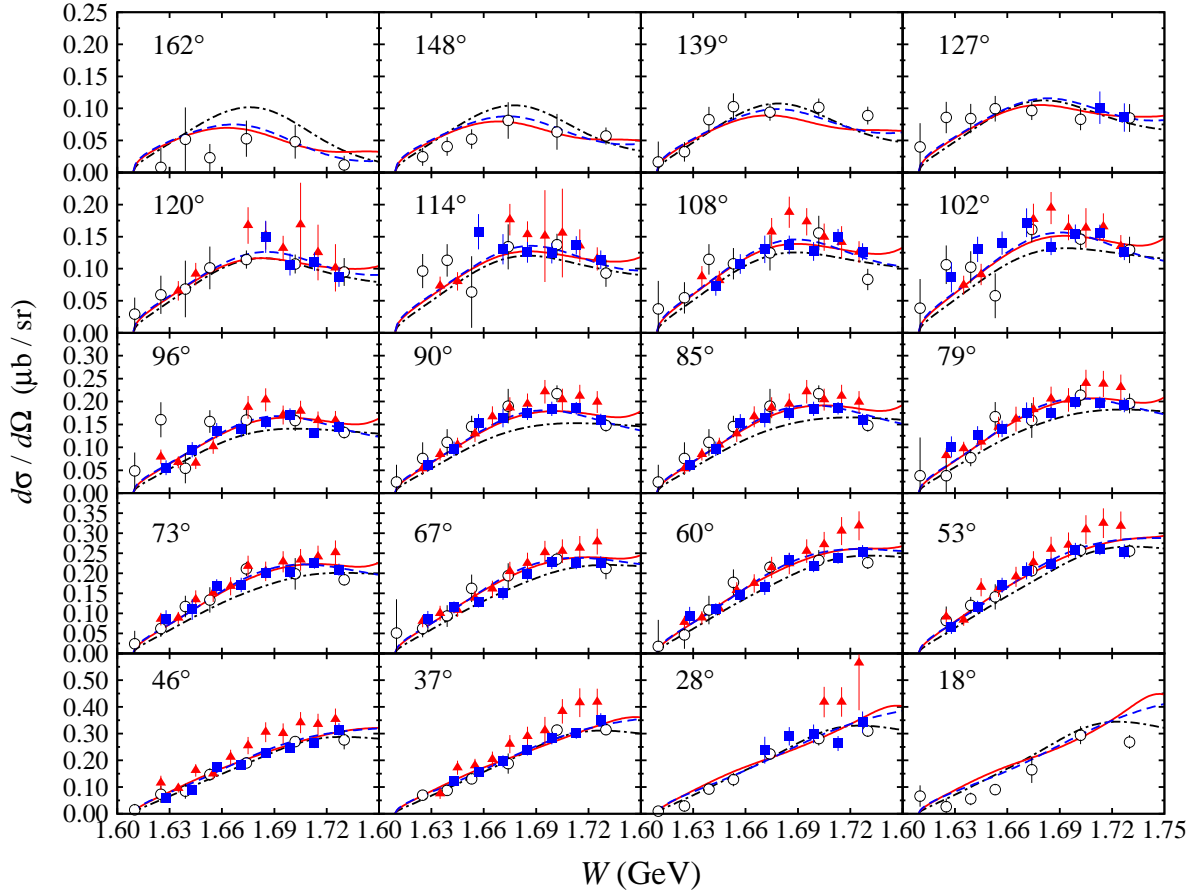


FIG. 5: (Color online) As in Fig. 4, but for the total c.m. energy distribution. The corresponding kaon scattering angle $\theta_K^{c.m.}$ is shown in each panel.

GeV can be observed. We note that within the error bars of the PDG resonance masses, all resonances considered in the present analysis could contribute to this bump. Besides that, the fact that threshold energies of all four $K\Sigma$ photoproductions are around 1.690 GeV, as shown in Table III, could also be the origin of this bump. Thus, we may conclude that an accurate extraction of resonance properties from kaon photoproduction at this energy point (1.690 GeV) would be a daunting task. The same situation could also happen at 1.720 GeV, at which both ρp and ωp photoproduction have their thresholds.

The Λ recoil polarization displayed in Fig. 6 reveals an interesting phenomenon, especially at $W = 1.625$ GeV (see Fig. 16 in the next section for the energy distribution of this structure). The present analysis, as well as the Kaon-Maid model, cannot reproduce the CLAS2010 data at this energy. We believe that, assuming the data are accurate, such

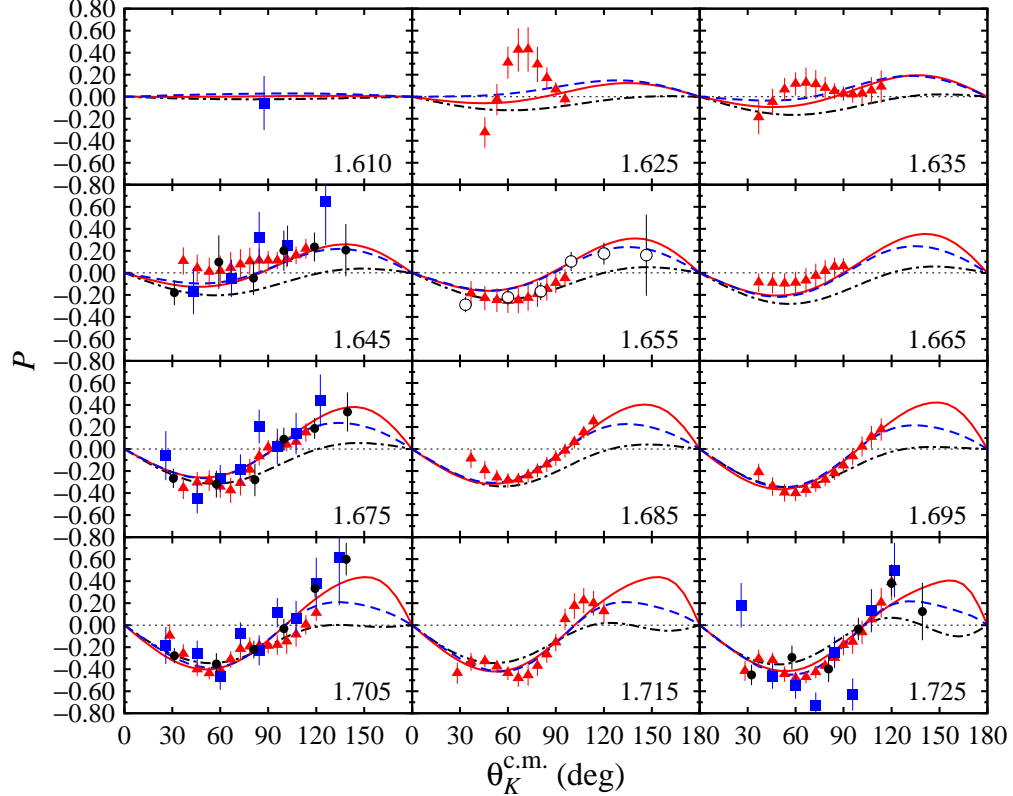


FIG. 6: (Color online) Recoil polarization calculated from Model 1, Model 2, and Kaon-Maid [21] compared with experimental data from the SAPHIR [19] (open circles), CLAS2006 (solid squares) [22], CLAS2010 (solid triangles) [26], and GRAAL [24] (closed circles) collaborations. Notation of the curves is as in Fig. 3. The corresponding total c.m. energy W (in GeV) is shown in each panel.

a structure cannot originate from an established nucleon resonance, since PDG does not listed any single resonance at $W = 1.625$ GeV. Since the polarization should be zero at threshold, such an obvious structure 15 MeV above the threshold requires special mechanism in the background terms that could dramatically change the polarization slightly above the production threshold. The probability that a "missing resonance" could solve this problem is very unlikely, since the cross sections shown in Figs. 3 and 5 do not indicate any structure at this energy region. At this stage we would just mention that future experimental and theoretical studies should address this problem as an important topic, since the polarization is automatically given in the kaon photoproduction experiments and, on the other hand, problems at the production threshold can be better solved by a more consistent mechanism such as chiral perturbation theory.

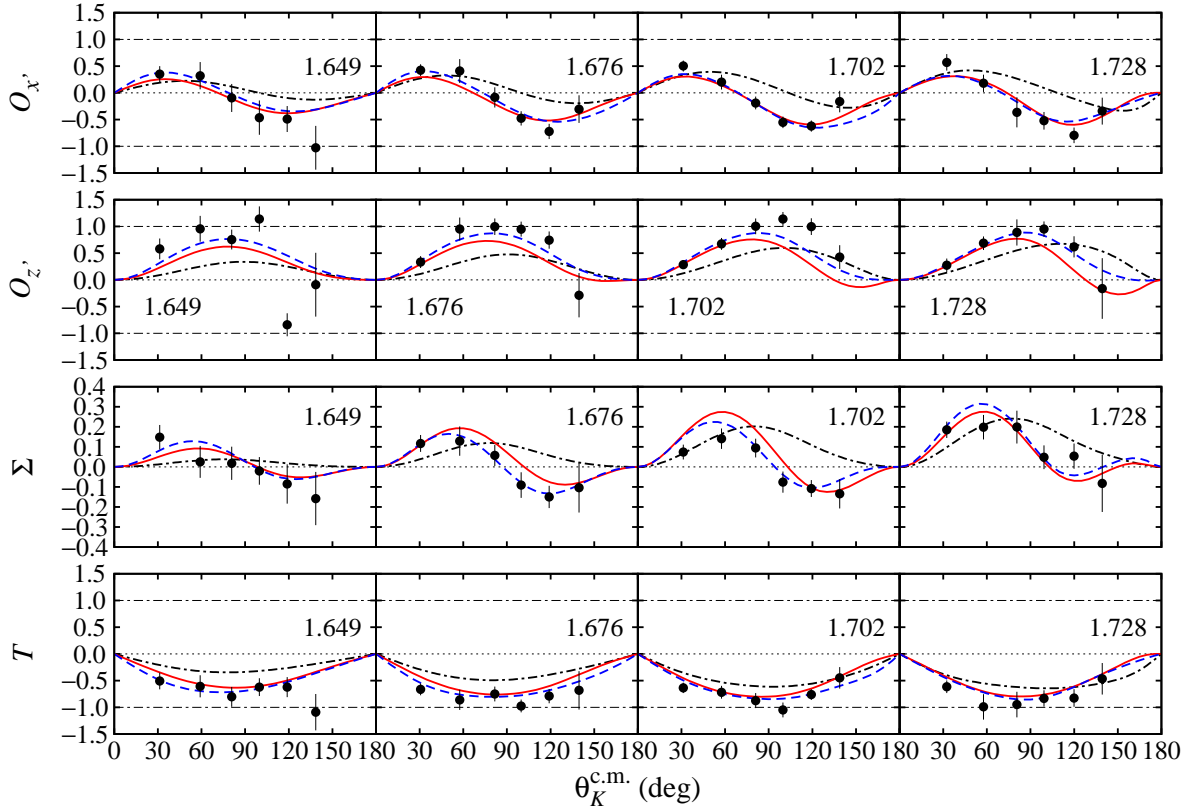


FIG. 7: (Color online) The beam-recoil double polarization observables $O_{x'}$ and $O_{z'}$, along with the target T and photon Σ asymmetries calculated from Model 1, Model 2, and Kaon-Maid models [21] compared with experimental data from the GRAAL [25] collaboration. Notation of the curves is as in Fig. 3.

The photon-, target-, and double-polarization observables $O_{x'}$, $O_{z'}$, C_x , C_z , are shown in Figs. 7 and 8. It is clear from these figures that both Model 1 and Model 2 can nicely describe the experimental data, although we should admit that Model 2 can reproduce the photon asymmetry data better than Model 1 due to its smaller χ^2 .

III. SEARCH FOR A NARROW RESONANCE IN KAON PHOTOPRODUCTION

Having extended our photoproduction model up to $W = 1730$ MeV, we are ready now to study the possibility of observing a narrow resonance in the $\gamma + p \rightarrow K^+ + \Lambda$ process. As discussed in the Introduction, in Ref. [7] an attempt to find the existence of a narrow $J^p = 1/2^+$ state was performed by including such a state in the πN partial wave P_{11} . The

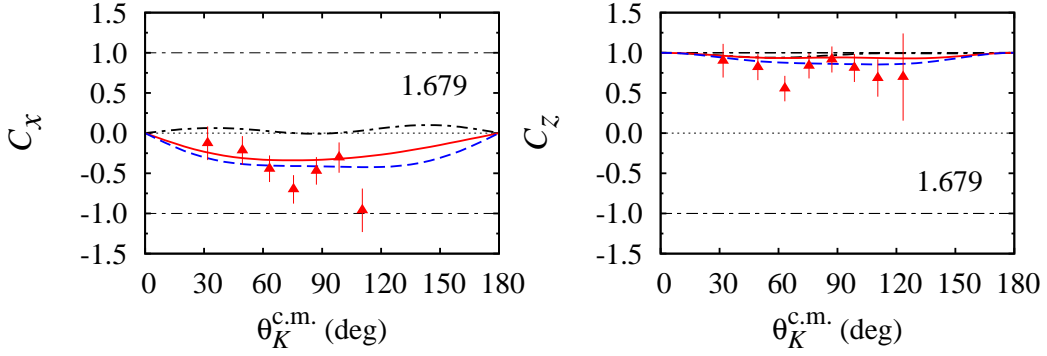


FIG. 8: (Color online) The beam-recoil observables C_x and C_z calculated from Model 1, Model 2, and Kaon-Maid models [21] compared with experimental data from Ref. [23]. Notation of the curves is as in Fig. 3.

TABLE III: Threshold energies of meson photoproductions around 1700 MeV in terms of the photon laboratory energy ($E_\gamma^{\text{thr.}}$) and the total c.m. energy ($W^{\text{thr.}}$). Note that the threshold energy of kaon photoproduction $\gamma + p \rightarrow K^+ + \Lambda$ is $E_\gamma^{\text{thr.}} = 911$ MeV ($W^{\text{thr.}} = 1609$ MeV).

No.	Channel	$E_\gamma^{\text{thr.}}$ (MeV)	$W^{\text{thr.}}$ (MeV)
1	$\gamma + p \rightarrow K^+ + \Sigma^0$	1046	1686
2	$\gamma + p \rightarrow K^0 + \Sigma^+$	1048	1687
3	$\gamma + n \rightarrow K^+ + \Sigma^-$	1052	1691
4	$\gamma + n \rightarrow K^0 + \Sigma^0$	1051	1690
5	$\gamma + p \rightarrow \rho + p$	1096	1714
6	$\gamma + p \rightarrow \omega + p$	1109	1721

change of overall χ^2 was scanned from $m_{N^*} = 1610$ to 1760 MeV. In the present work we follow this method, i.e., we include an extra narrow P_{11} resonance state in the kaon photoproduction amplitude and scan the changes in the total χ^2 after the inclusion, in the energy range where our model is valid, i.e., $W = 1620$ to 1730 MeV. Note that we do not start the scan from $m_{N^*} = 1610$ MeV, since the cross section at this threshold energy is very small, while experimental data have very large error bars (see the first panel of Fig. 4). As a consequence, predictions of our model at this kinematics would be less reliable. The same

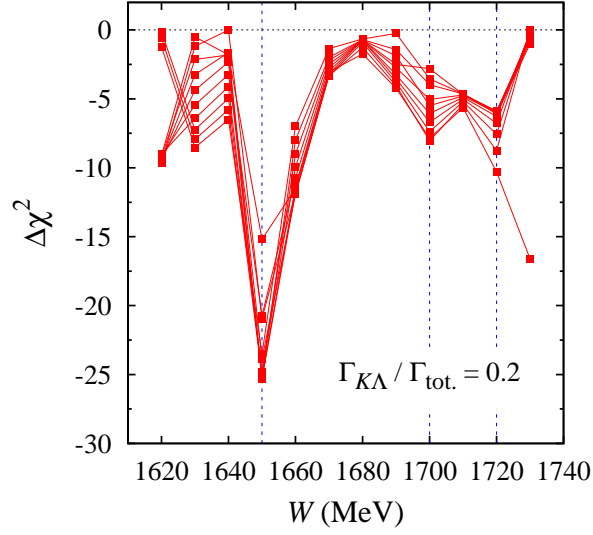


FIG. 9: (Color online) Change of the χ^2 in the fit of Model 1 due to the inclusion of the P_{11} resonance with the mass scanned from 1620 to 1730 MeV (step 10 MeV) and $\Gamma_{\text{tot.}}$ taken from 1 to 10 MeV (step 1 MeV) for the $K\Lambda$ branching ratio 0.2. The three vertical lines indicate $m_{N^*} = 1650$, 1700 and 1720 MeV. A similar result is obtained for the $K\Lambda$ branching ratio 0.1 and 0.4.

behavior is also observed at the upper energy limit of the present analysis (1730 MeV).

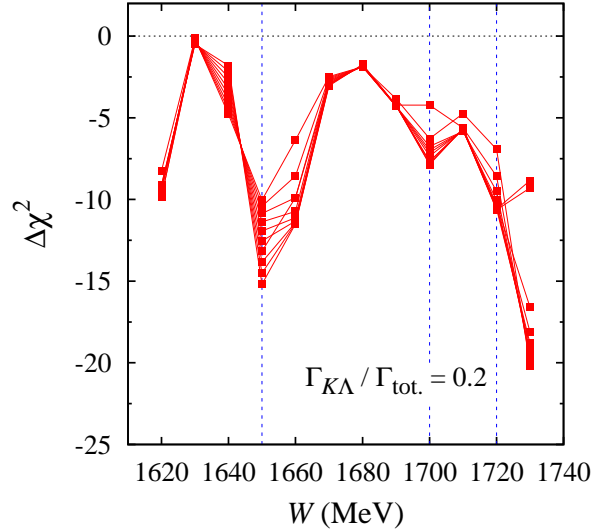


FIG. 10: (Color online) As in Fig. 9, but calculated by using total widths $\Gamma_{\text{tot.}}$ from 0.1 to 1 MeV (step 0.1 MeV).

Figure 9 displays the result of χ^2 changes ($\Delta\chi^2$) after the inclusion of an extra P_{11} resonance in Model 1 with the mass scanned from 1620 to 1730 MeV, where the total width is varied from 1 to 10 MeV with 1 MeV step. Although not shown in the figure, we have also investigated the effect of the variation of $K\Lambda$ branching ratio and found only a small effect on the $\Delta\chi^2$. From Fig. 9 we can see that three minima appear at $m_{N^*} = 1650, 1700,$ and 1720 MeV. Nevertheless, the minimum $\Delta\chi^2$ at $m_{N^*} = 1650$ MeV seems to be the most convincing one. For all values of the $K\Lambda$ branching ratio investigated in this study the lowest values of $\Delta\chi^2$ can be obtained by using $\Gamma_{\text{tot.}} = 5$ MeV. Variation of the total width $\Gamma_{\text{tot.}}$ results in a variation of the $\Delta\chi^2$ value.

As in Ref. [7], we have also repeated our calculation by using the total width varying from 0.1 to 1 MeV with 0.1 MeV step. The result is shown in Fig. 10. Although the absolute values of $\Delta\chi^2$ obtained in this case are significantly different from those in the previous case, the similar pattern still appears. Only at $m_{N^*} = 1720$ MeV the minimum value of $\Delta\chi^2$ seems to disappear, since $\Delta\chi^2$ further decreases at $m_{N^*} = 1730$ MeV. This is due to the fact that our model is less reliable at the upper energy limit (see total and differential cross sections shown in Figs. 3 and 5). As in the previous case, variation of the total width yields variation of the $\Delta\chi^2$ and variation of the branching ratio changes this result slightly. Note that the absolute values of $\Delta\chi^2$ here are smaller than in the case of larger $\Gamma_{\text{tot.}}$. Therefore, at this stage we may conclude that our result prefers the total width values in the range of $1 \text{ MeV} \leq \Gamma_{\text{tot.}} \leq 10 \text{ MeV}$.

To investigate model dependence of our result in Fig. 11 we display the same result as in Fig. 9 with a branching ratio of 0.1, but using Model 2. Once again, we see a similar pattern found in Fig. 10. We, therefore, conclude that the minimum at $m_{N^*} = 1650$ seems to be model independent, whereas the minima at 1700 and 1720 MeV seem to disappear in Model 2. This phenomenon can be understood from the fact that Model 2 has smaller χ^2 , i.e., the agreement with experimental data is better than in Model 1. Thus, improvement of the χ^2 by adding nucleon resonances is less likely in Model 2. As a consequence, the number of minima in Model 2 is significantly reduced. To check this argument, we have also analyzed a model that makes use of nucleon resonances found in the analysis of new pion photoproduction data from the CLAS collaboration [28]. In this analysis only the $S_{11}(1650), D_{15}(1675), F_{15}(1680),$ and $P_{13}(1720)$ states are considered, whereas the variation of resonance parameters is very limited. Obviously, the agreement with kaon photoproduction data is worse ($\chi^2/N = 1904$)

than in Model 1 ($\chi^2 = 859$) or Model 2 ($\chi^2 = 704$). As a consequence, four minima are observed in the plot of $\Delta\chi^2$, i.e., at 1650, 1670, 1690, and 1720 MeV, which clearly supports our argument above.

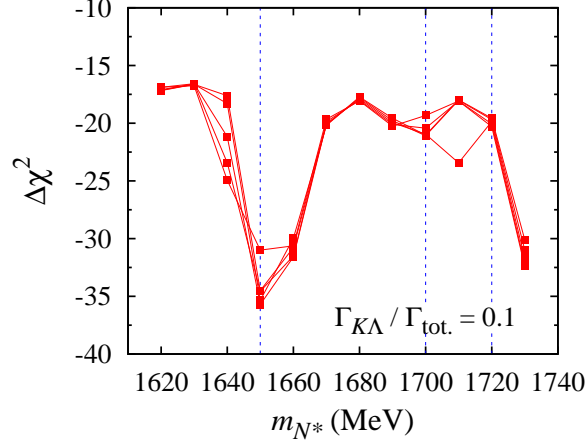


FIG. 11: (Color online) As in Fig. 9, but for Model 2 with the $K\Lambda$ branching ratio 0.1.

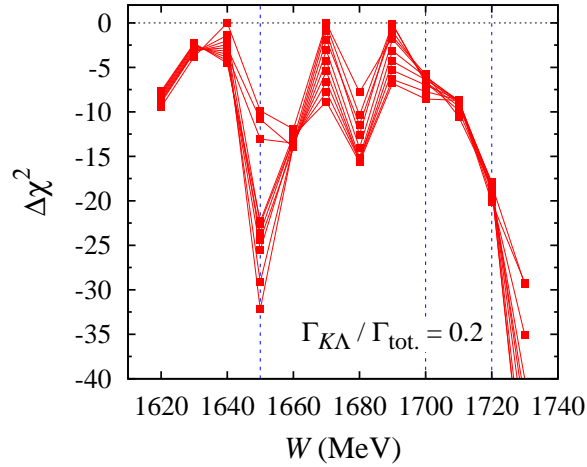


FIG. 12: (Color online) Change of the χ^2 in the fit of Model 1 due to the inclusion of the S_{11} resonance with the mass scanned from 1620 to 1730 MeV (step 10 MeV) and using $\Gamma_{\text{tot.}}$ from 1 to 10 MeV (step 1 MeV) for the $K\Lambda$ branching ratio 0.2. As in Fig. 9, the three vertical lines indicate $m_{N^*} = 1650, 1700$ and 1720 MeV. Note that a new minimum at 1680 MeV appears in this case.

Our finding corroborates the result of the topological soliton model of Walliser and Kopelevich [2] discussed in the Introduction of this paper. The χ QSM of Diakonov and Petrov

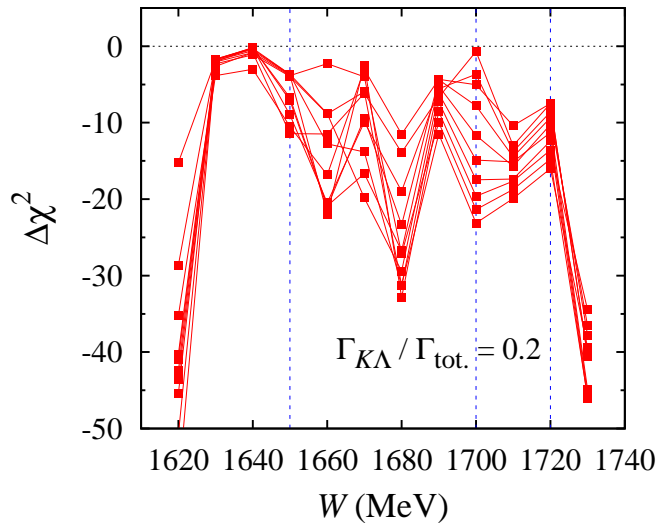


FIG. 13: (Color online) As in Fig. 12, but for the case of P_{13} .

[6] predicts a $J^P = 1/2^+$ N^* state with a mass around 1650 MeV if the possible mixing between the lower-lying nucleonlike octet with the antidecuplet is neglected. Thus, our result seems to support this possibility. Although our finding does not exclude the possibility that a narrow P_{11} resonance with a mass of 1700 or 1720 MeV could exist, we believe that investigation of the resonance effects at these energies by using the present mechanism is difficult due to the opening of $K\Sigma$, ρp , and ωp channels.

IV. ORIGIN OF THE MINIMA AND POSSIBILITY OF OTHER RESONANCE STATES

Although in this paper we have assumed the existence of a narrow P_{11} resonance as predicted by the χ QSM and we only intent to explore the possibility that it exists in the kaon photoproduction reaction, the results found in the previous section could be also obtained by using other resonances, e.g., an S_{11} or a P_{13} . As discussed in the Introduction, a similar situation has been also found in the η photoproduction [13]. To clarify this problem, in Fig. 12 we plot the changes of the χ^2 if we replace the P_{11} narrow resonance in the amplitude of Model 1 with an S_{11} ($J^P = 1/2^-$) resonance. Obviously the same minimum at $m_{N^*} = 1650$ MeV is retained, but a new one clearly appears at $m_{N^*} = 1680$ MeV. The appearance of the minimum $\Delta\chi^2$ at $m_{N^*} = 1650$ MeV in all $\Delta\chi^2$ shown by Figs. 9 – 12 indicates

that a real structure really exists at this energy, although it is hardly seen in experimental data. However, the fact that both S_{11} and P_{11} could generate this minimum means that a $J^p = 1/2^-$ narrow resonance is also possible in the kaon photoproduction process.

Figure 13 displays the change of the χ^2 in the fit of Model 1 if we include a P_{13} ($J^p = 3/2^+$) narrow resonance instead of an S_{11} or a P_{11} state. Surprisingly, the minimum at 1650 MeV almost vanishes and a clear minimum at 1680 MeV, as in the case of the S_{11} , appears. Besides that we also observe two weaker minima at 1660 and 1700 MeV. However, the minimum at 1680 MeV is interesting in this case, since the possibility that the structure found in the η photoproduction off a neutron can be explained by a P_{13} resonance has been discussed in Ref. [8]. In fact, the most convincing result with the smallest χ^2 would be obtained if one used a $P_{13}(1685)$ state instead of a P_{11} state [8]. Unfortunately, as discussed above and shown in Table III, at energies around 1685 MeV there exists a number of meson photoproduction thresholds. Therefore, unless we could suppress the threshold effects at this energy point, further discussion of the $P_{13}(1685)$ would be meaningless at this stage.

In the PWA it is possible to check whether the true resonance extracted from the analysis is a P_{11} or not. A true resonance would yield an effect only when inserted into the correct partial amplitude [7]. In the present analysis such a technology is unfortunately not available. However, in principle, different natures of the P_{11} , S_{11} , and P_{13} resonances represented by their different formulations are traceable in the measured observables.

To prove this argument, in Fig. 14 we show different effects generated by the P_{11} and

TABLE IV: Extracted narrow resonance parameters in the case that the resonance is an S_{11} , a P_{11} , or a P_{13} state. The S_{11} and P_{11} parameters are used in the following discussion, whereas the P_{13} parameters are given just for comparison.

Extracted parameters	S_{11}	P_{11}	P_{13}
$A_{1/2}$ (10^{-3} GeV $^{1/2}$)	+90	+40	-19
$A_{3/2}$ (10^{-3} GeV $^{1/2}$)	-	-	+80
m_{N^*} (MeV)	1650	1650	1680
$\Gamma_{\text{tot.}}$ (MeV)	6	5	8
β_K	0.2	0.2	0.2
ϕ (deg.)	64	67	0

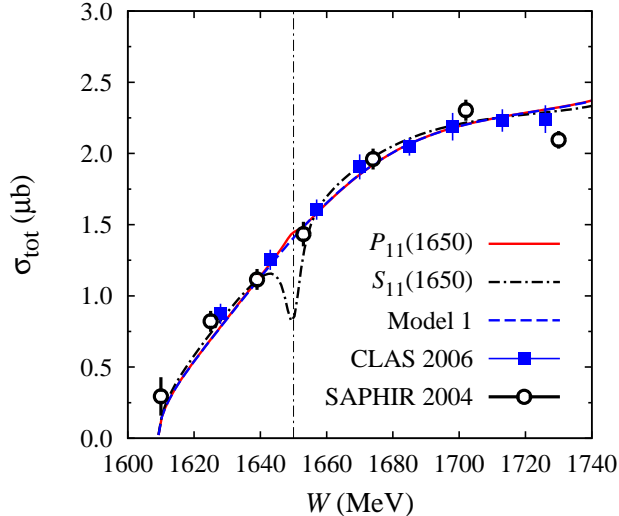


FIG. 14: (Color online) Effects of the inclusion of P_{11} and S_{11} resonances with resonance parameters given in Table IV on the total cross section of the $\gamma + p \rightarrow K^+ + \Lambda$ process.

the S_{11} resonances on the total cross section compared with experimental data. Note that we use the resonance parameters given in Table IV, which are obtained as the best fits to experimental data. Interestingly, the S_{11} resonance generates a clear dip at $W = 1650$ MeV in the total cross section, whereas the effect of the P_{11} resonance is almost negligible. Clearly, such a dip is not observed by the presently available data, since the energy bin of the data is larger than the width of the dip. Should the structure around 1650 MeV really exist, then future experiments with smaller energy bins (e.g. 2 MeV) would be required to resolve it and, simultaneously, to single out the true resonance.

How can the structure predicted by the $\Delta\chi^2$ minima in Figs. 9 – 12 almost disappear in the total cross section? The answer is given in Fig. 15, where we can see that the effect of the P_{11} resonance on the differential cross sections is in fact comparable with that of the S_{11} resonance, but the effect changes almost drastically at $\theta_K^{c.m.} \approx 70^\circ$ from decreasing to increasing cross section as the kaon angle increases. This phenomenon obviously disappears in the total cross section after an angular integration over all possible angles averages this effect. In the case of the S_{11} we obtain a decreasing effect in the whole angular distribution, which therefore produces an obvious dip at $W = 1650$ MeV in the total cross section.

It is obviously important to know which data are really responsible for the minimum at 1650 MeV as shown in Figs. 9 – 12. For this purpose, we have scrutinized contributions of

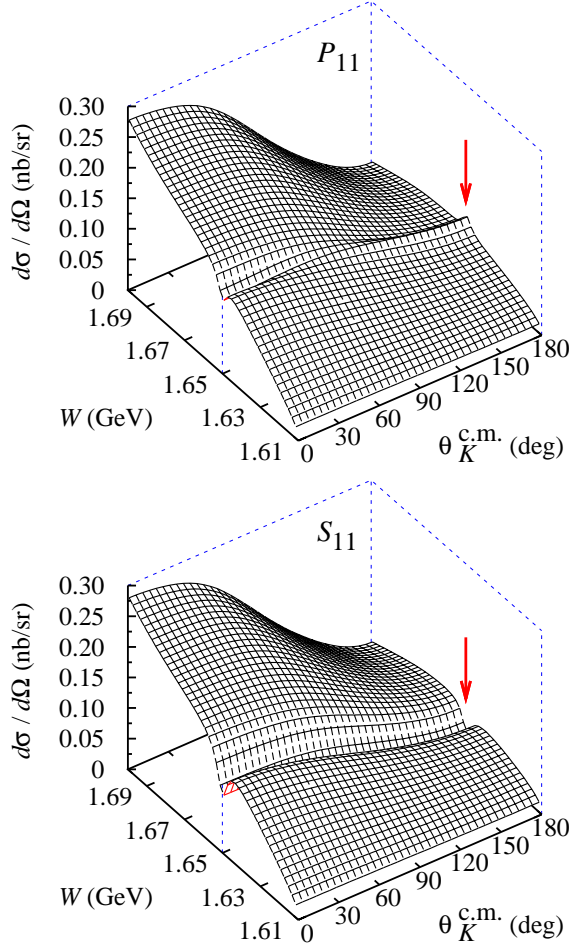


FIG. 15: (Color online) Effects of the inclusion of the P_{11} (top figure) and S_{11} (bottom figure) resonances with resonance parameters given in Table IV on the differential cross sections. Arrows in the figures indicate the position of $W = 1.650$ GeV.

individual data to the χ^2 in our fits and found that this minimum originates mostly from the Λ recoil polarization data as displayed in Fig. 16. From this figure we can see that there exists a dip at $W \approx 1650$ MeV in the whole angular distribution of data. It is also apparent that both P_{11} and S_{11} states can nicely reproduce the dip. Therefore, it seems to us that the recoil polarization is not the suitable observable to distinguish the possible states at 1650 MeV. Nevertheless, more precise recoil polarization data are still urgently required in order to support the finding of the present work as well as to remove uncertainties in the position of the dip. Definitely, JLab FROST project looks promising for this purpose [29].

In the beam-recoil double polarization observables $O_{x'}$ and $O_{z'}$ the presence of an S_{11} or

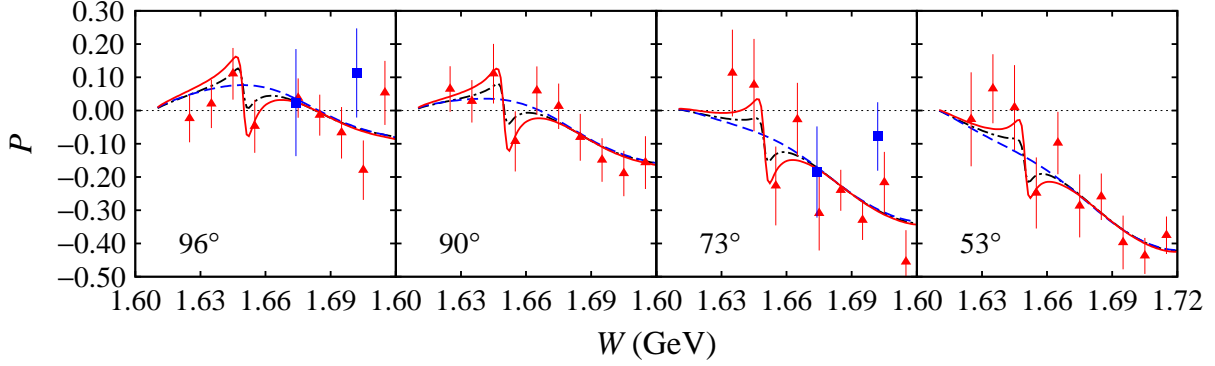


FIG. 16: (Color online) As in Fig. 14, but for the Λ recoil polarization. Notation for the experimental data is as in Fig. 6.

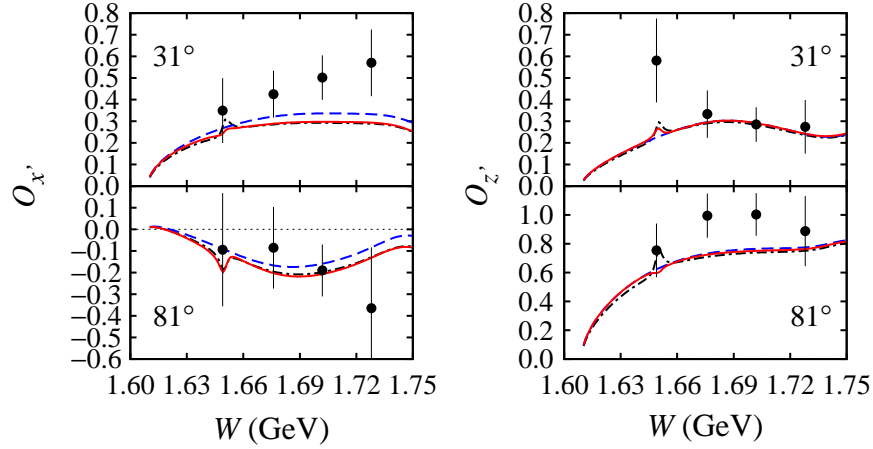


FIG. 17: (Color online) As in Fig. 14, but for the $O_{x'}$ and $O_{z'}$ double polarization observables. Experimental data are from the GRAAL [25] collaboration.

a P_{11} narrow state predicts a small structure at 1650 MeV. In the case of the S_{11} state the structure is slightly more obvious than in the case of the P_{11} state. We note that for the $O_{x'}$ observable this structure increases as the kaon angle increases. The opposite behavior is shown by the $O_{z'}$ observable. Although the structures seem to be mild, their differences generated by the different natures of the S_{11} and P_{11} resonances might provide important observables to determine the origin of the $\Delta\chi^2$ minimum at 1650 MeV.

Although the effect is milder, the same behavior is also shown by the target asymmetry T , as exhibited in Fig. 18. In the case of photon asymmetry, given in the same figure, the

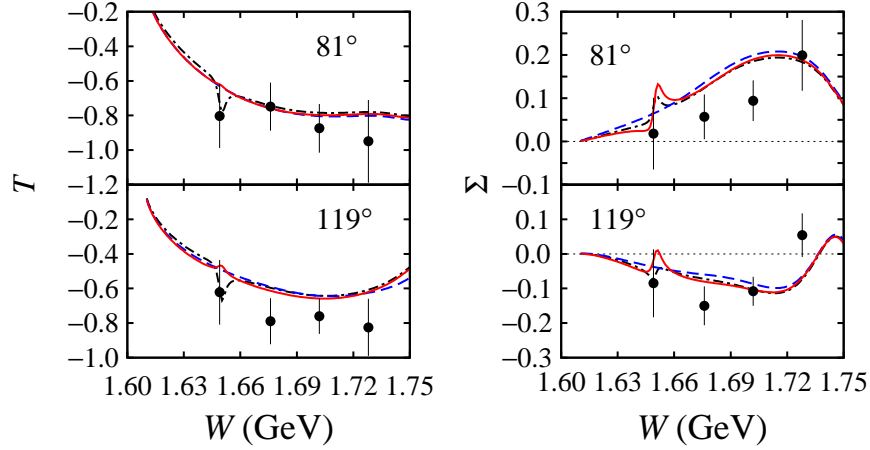


FIG. 18: (Color online) As in Fig. 17, but for the target and photon beam asymmetry.

effect generated by the P_{11} states is more obvious than that by the S_{11} state.

The effect of the narrow resonances is also found to be sizable on the beam-recoil double polarization observables C_x and C_z , as displayed in Fig. 19. Different from the photon or beam-recoil asymmetries, Σ and $O_{z'}$, here we observe that both resonances yield a clear dip at $W = 1650$ MeV. Although C_x and C_z probably cannot distinguish the effects of S_{11} and P_{11} states, the sizable dips produced here indicate that these observables are seem to be promising for investigation of the narrow resonance existence in kaon photoproduction.

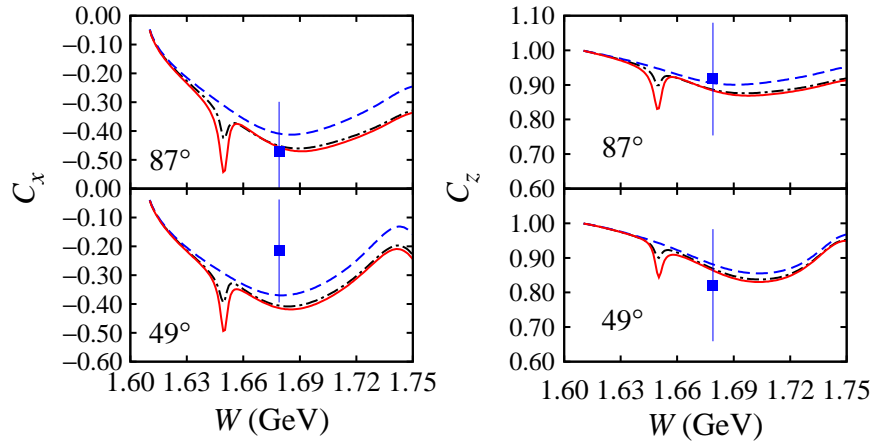


FIG. 19: (Color online) As in Fig. 14, but for the C_x and C_z double polarization observables. Experimental data are from Ref. [23].

We believe that new measurements with the present accelerator and detector technologies would be able to resolve the effects shown in Figs. 14 and 15. Furthermore, more precise kaon photoproduction data with energy bins about 2 MeV would be already able to discriminate the effect of P_{11} and S_{11} resonances on the total cross section and improve the accuracy of our calculation.

V. SUMMARY AND CONCLUSION

We have studied the possibility of observing the $J^p = 1/2^+$ narrow resonance, the non-strange member of antidecuplet baryons predicted by the χ QSM, in kaon photoproduction off a proton. For this purpose, we have constructed two isobar models that can reproduce experimental data from threshold up to $W = 1730$ MeV, based on our previous effective Lagrangian model. After inserting the resonance in the models we analyzed the changes in the total χ^2 with the variation of m_{N^*} from 1620 to 1730 MeV and found the most convincing minimum at $m_{N^*} = 1650$ MeV. This finding is observed for all isobar models used in this investigation and could be distinguished from the $J^p = 1/2^-$ and $3/2^+$ resonances, provided that more precise kaon photoproduction data were available. Furthermore, our conclusion does not change with the variation of the total width and $K\Lambda$ branching ratio of the resonance. Although the mass of the resonance obtained in our calculation (i.e., 1650 MeV) is slightly different from those obtained from the πN and ηN reactions, the 1650 MeV mass corroborates the result of the topological soliton model and the calculation utilizing the Gell-Mann-Okubo rule without mixing between the lower-lying nucleonlike octet with the antidecuplet. Needless to say that more precise kaon photoproduction data are crucial to prove and improve our present calculation.

Acknowledgment

The author thanks Igor I. Strakovsky for suggesting this study and for fruitful discussions. Supports from the University of Indonesia and the Competence Grant of the Indonesian

Ministry of National Education are gratefully acknowledged.

- [1] D. Diakonov, V. Petrov, and M. Polyakov, *Z. Phys. A* **359**, 305 (1997).
- [2] H. Walliser and V. B. Kopeliovich, *J. Exp. Theor. Phys.* **97**, 433 (2003) [*Zh. Eksp. Teor. Fiz.* **124**, 483 (2003)].
- [3] R. M. Barnett *et al.*, *Phys. Rev. D* **54**, 1 (1996).
- [4] C. Alt *et al.*, *Phys. Rev. Lett.* **92**, 042003 (2004).
- [5] T. Nakano *et al.*, *Phys. Rev. Lett.* **91**, 012002 (2003).
- [6] D. Diakonov and V. Petrov, *Phys. Rev. D* **69**, 094011 (2004).
- [7] R. A. Arndt, Ya. I. Azimov, M. V. Polyakov, I. I. Strakovsky, and R. L. Workman, *Phys. Rev. C* **69**, 035208 (2004).
- [8] V. Kuznetsov *et al.*, *Phys. Lett. B* **647**, 23 (2007).
- [9] F. Miyahara *et al.*, *Prog. Theor. Phys. Suppl.* **168**, 90 (2007); I. Jaegle *et al.*, *Phys. Rev. Lett.* **100**, 252002 (2008).
- [10] A. Fix, L. Tiator and M. V. Polyakov, *Eur. Phys. J. A* **32**, 311 (2007).
- [11] M. Doring and K. Nakayama, *Phys. Lett. B* **683**, 145 (2010).
- [12] V. Skhlyar, H. Lenske and U. Mosel, *Phys. Lett. B* **650**, 172 (2007).
- [13] K. S. Choi, S. i. Nam, A. Hosaka, and H.-Ch. Kim, *Phys. Lett. B* **636**, 253 (2006).
- [14] R.A. Arndt, W.J. Briscoe, M.W. Paris, I.I. Strakovsky, R.L. Workman, *Chin. Phys. C* **33**, 1063 (2009); arXiv:0906.3709 [nucl-th].
- [15] T. Mart, *Phys. Rev. C* **82**, 025209 (2010).
- [16] T. Mart and A. Sulaksono, *Phys. Rev. C* **74**, 055203 (2006).
- [17] H. Haberzettl, C. Bennhold, T. Mart and T. Feuster, *Phys. Rev. C* **58**, 40 (1998).
- [18] M. Bockhorst *et al.*, *Z. Phys. C* **63**, 37 (1994); M. Q. Tran *et al.*, *Phys. Lett. B* **445**, 20 (1998).
- [19] K. H. Glander *et al.*, *Eur. Phys. J. A* **19**, 251 (2004).
- [20] K. Nakamura *et al.* (Particle Data Group), *J. Phys. G* **37**, 075021 (2010).
- [21] T. Mart, C. Bennhold, H. Haberzettl, and L. Tiator, Kaon-Maid. The interactive program is available at <http://www.kph.uni-mainz.de/MAID/kaon/kaonmaid.html>. The published versions are available in: T. Mart and C. Bennhold, *Phys. Rev. C* **61**, 012201 (1999); T. Mart, *Phys. Rev. C* **62**, 038201 (2000); C. Bennhold, H. Haberzettl and T. Mart,

arXiv:nucl-th/9909022.

- [22] R. Bradford *et al.*, Phys. Rev. C **73**, 035202 (2006).
- [23] R. Bradford *et al.*, Phys. Rev. C **75**, 035205 (2007).
- [24] A. Lleres *et al.*, Eur. Phys. J. A **31**, 79 (2007).
- [25] A. Lleres *et al.*, Eur. Phys. J. A **39**, 146 (2009).
- [26] M. E. McCracken *et al.*, Phys. Rev. C **81**, 025201 (2010).
- [27] M. Q. Tran *et al.*, Phys. Lett. B **445**, 20 (1998).
- [28] M. Dugger *et al.*, Phys. Rev. C **79**, 065206 (2009).
- [29] Further information about the Jefferson Lab Frozen Spin Target (FroST) experiment can be found at <http://www.jlab.org/~ckeith/Frozen/Frozen.html>